# Prediction of Broadband Noise from Horizontal Axis Wind Turbines

Ferdinand W. Grosveld*
*The Bionetics Corporation, Hampton, Virginia*

**A method is presented for predicting the broadband noise spectra of horizontal axis wind turbine generators. It includes contributions from such noise sources as the inflow turbulence to the rotor, the interactions between the turbulent boundary layers on the blade surfaces with their trailing edges, and the wake due to a blunt trailing edge. The method is partly empirical and is based on acoustic measurements of large wind turbines and airfoil models. The predicted frequency spectra are compared with measured data from several machines, including the MOD-OA, MOD-2, WTS-4, and U.S. Windpower Inc. machine. The significance of the effects of machine size, power output, trailing-edge bluntness, and distance to the receiver is illustrated. Good agreement is obtained between the predicted and measured far-field noise spectra.**

## Nomenclature

$B$ = number of blades
$c$ = chord
$c_o$ = speed of sound
$c_r$ = root chord
$c_t$ = tip chord
$C_L$ = lift coefficient
$D$ = blade diameter
$\bar{D}$ = directivity
$f$ = frequency
$F$ = force
$G(k)$ = aerodynamic transfer function
$h$ = elevation above ground level
$i$ = $\sqrt{-1}$
$k$ = wavenumber ($\omega c_o/2V_w$)
$K_2$ = scaling factor
$K_j(f)$ = frequency dependent scaling factor, ($j=1,3,4$)
$\ell$ = spanwise length of blade segment
$L$ = lift force
$M$ = Mach number
$M_c$ = convection Mach number
$n$ = revolutions per second
$p$ = acoustic far-field pressure
$P$ = power
$P_r$ = rated power
$Q$ = torque
$r_o$ = distance between source and receiver
$r_x$ = distance from local blade section to center of hub
$\bar{r}$ = vector from source to receiver location
$R$ = rotor blade radius
$R_N$ = Reynolds number
$s$ = airfoil span
$S$ = Strouhal number
$\mathrm{SPL}_{1/3}$ = one-third octave band sound pressure level
$t$ = time
$U$ = freestream velocity
$V_c$ = convection speed
$V_{ci}$ = cut-in wind speed
$V_r$ = rated wind speed
$V_w$ = wind speed
$w_r$ = reference turbulence intensity
$\bar{w}$ = square root of the mean square turbulence intensity
$x$ = vertical coordinate
$y$ = horizontal coordinate
$z$ = downwind coordinate
$\alpha$ = angle of attack
$\beta$ = geometric pitch angle
$\gamma$ = aerodynamic pitch angle
$\delta$ = boundary-layer thickness
$\delta^*$ = boundary-layer displacement thickness
$\eta$ = reduced frequency ($\omega h/V_w$)
$\theta$ = angle between source-receiver line (in vertical plane) and its projection in the rotor plane
$\dot{\theta}$ = rotor rate
$\nu$ = kinematic viscosity
$\rho$ = air density
$\phi$ = angle between vector $\bar{r}$ and its projection in the rotor plane
$\Phi_z$ = longitudinal turbulence spectrum
$\psi$ = angle between source-receiver line and the horizontal in the rotor plane
$\omega$ = rotational frequency

Received Aug. 30, 1984; presented as Paper 84-2357 at the AIAA/NASA 9th Aeroacoustics Conference, Oct. 15-17, 1984, Williamsburg, Va.; revision received Jan. 16, 1985. 

*Aero-Space Research Engineer. Senior Member AIAA.

## Introduction

TO adequately assess the impact of the wind turbine noise and to aid in the design and siting of machines that are acceptable to the community,[1,2] a thorough understanding of the underlying noise generation phenomena as well as prediction techniques are necessary. Most available publications on wind turbine noise deal with the impulsive "thumping" noise caused by the rotor blades cutting the wake behind their supporting tower, where the rotor is located downwind from the tower.[3-9] A prediction code for this type of low-frequency noise is presented in Ref. 10. Other possible sources of wind turbine broadband noise are discussed in Ref. 11 and some of those noise mechanisms are considered in Refs. 12-16. Comparison of theory with experimental broadband noise data[12,17] as presented in Ref. 16 indicates that more accurate prediction techniques are needed. The purpose of this research is to present and discuss a method to predict the broadband noise from horizontal axis wind turbines and to compare the results with measured data from currently operating machines.

## Broadband Noise Prediction

Extensive noise measurements on current horizontal axis wind turbine generators[11-13,17-19] indicate the presence of three major aerodynamic source mechanisms of broadband noise:

1) Loading fluctuations due to the inflow turbulence interacting with the rotating blades.

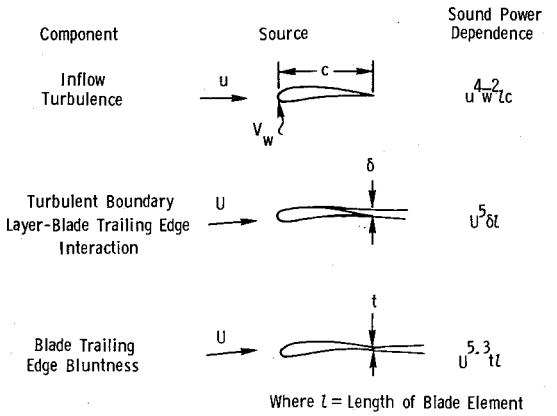


**Fig. 1 Components of wind turbine broadband noise.**

2) The turbulent boundary-layer flow over the airfoil surface interacting with the blade trailing edge.

3) Vortex shedding due to trailing-edge bluntness.

The components of wind turbine broadband noise are illustrated in Fig. 1.

In contrast to the limited literature on wind turbine noise, the list of publications dealing with helicopter rotor noise is quite extensive.[22,23] Although the concept of extracting energy from the flow by a wind turbine rotor is opposite that of a helicopter rotor, which provides energy to the flow, the noise generating mechanisms show many similarities and an analogy between the two concepts is justified.

### Inflow Turbulence

When the wind turbine rotor blades move through the turbulent air, they encounter atmospheric inhomogeneities causing effective changes in the angle of attack that result in unsteady airfoil loading. This fluctuating force mechanism is a well-known source for airfoil and helicopter rotor noise.[16,22-37] To enable utilization of theoretical analyses from the literature for turbulent inflow source mechanisms applicable to helicopter rotors, the contrast with wind turbine rotor mechanisms has to be discussed. When encountering inflow turbulence, a helicopter rotor will ingest the turbulent eddy with a convection speed $V_c$, while for a wind turbine the eddy is blown into its rotor disk with a wind speed $V_w$. Downstream of the rotor plane of the wind turbine, the flow is slowed and the eddy compressed. The lifting rotor of a helicopter accelerates the flow and the eddies are elongated. If the eddies are compressed rather than elongated and if the blade passage frequency is kept constant, the occurence of blade loading correlation due to the chopping of a single eddy by more than one blade is reduced.

#### *Turbulence Characteristics*

The length scale and the intensity of the inflow turbulence are dependent on meteorological conditions and height above the ground.[38] A helicopter flying at different altitudes will thus encounter different turbulence conditions, while for any given wind turbine the distance above the ground is fixed. For the wind turbines considered here, the turbulence might be considered isotropic, which means that fluctuations are approximately the same in all directions.[39] For horizontal axis wind turbine generators, the longitudinal turbulence component is by far the most important. This longitudinal component is assumed to be a horizontal sinusoidal gust of the form

$$w = \bar{w} e^{i\omega(t - z/V_w)} \tag{1}$$

The wind structure is strongly dependent on the temperature gradient and the turbulence is sensitive to the state of the atmosphere and general meteorological conditions. In this study, neutral atmospheric stability conditions are assumed, with a negative temperature gradient as a function of the height above the ground. The mean square turbulence intensity at elevation $h$ is given by[40]

$$\bar{w}^2 = \int \Phi_z \, d\omega \tag{2}$$

where $\Phi_z$ is the average longitudinal turbulence spectrum and is expressed in terms of a reference turbulence intensity[40] $w_r$

$$\Phi_z(\eta, V_w) = \frac{w_r^2}{\omega}\left[\frac{0.164\eta/\eta_o}{1+0.164(\eta/\eta_o)^{5/3}}\right] \tag{3}$$

As used in the structural analysis of the MOD-2 machine, the reference turbulence intensity is defined by[40]

$$w_r = 0.2[2.18 V_w h^{-0.353}]^{1/(1.185-0.193\log h)} \tag{4}$$

Substitution of Eq. (3) in Eq. (2) yields, after integration, the root mean square turbulence intensity as a function of only wind speed and height above the ground,

$$\bar{w}^2 = w_r^2\{hw_r/[V_w R(w_r - 0.014 w_r^2)]\}^{-2/3} \tag{5}$$

The longitudinal turbulence spectrum $\Phi_z$ has been integrated between a minimum frequency chosen very close to zero and a maximum frequency $\omega_{\max}$ chosen such that high-frequency (small extent) turbulence may be disregarded.[40]

#### *Far-Field Noise Prediction*

The induced fluctuating force $\partial F/\partial t$ per unit span is related to the horizontal gust by the aerodynamic transfer function $G(k)$,

$$\left(\frac{\partial F}{\partial t}\right)^2 = \omega^2 \bar{w}^2 e^{2i\omega(t - z/V_w)} |G(k)|^2 \tag{6}$$

where $G(k)$ is based on Osborne's asymptotic solution for the compressible extension of the Sears function,[27,31] which for low-frequencies is approximated by

$$G(k) = \pi \rho U c \, dr/(1 + 2\pi k) \tag{7}$$

Lighthill[41] has shown that the sound pressure due to a fluctuating force $F_i$ at a point with coordinates $x_i$ $(i = 1,2,3)$ is given by the expression

$$p(t) - p_o = \frac{x_i}{4\pi r_o^2}\left[\frac{1}{c_o}\frac{\partial F_i(t - r_0/c_0)}{\partial t} + \frac{1}{r_o} F_i(t - r_0/c_0)\right] \tag{8}$$

If the source is considered to be a point dipole and the wavelength of the radiated sound is much smaller than the distance $r_o$ to the receiver, the expression for the acoustic pressure in the far field formulated by Curle[42] may be used,

$$p(\bar{r}, t) = \frac{\sin\phi}{4\pi c_o r_o}\int \frac{\partial F(t - r_0/c_0)}{\partial t} \tag{9}$$

where $\bar{r}$ is the vector from the source to the receiver location and $\phi$ the angle between $\bar{r}$ and its projection in the rotor plane. Substituting Eqs. (6) and (7) into Eq. (9) yields, after integration and squaring, the mean square sound pressure in the far field

$$|p^2| = K_1(f) B \sin^2\phi \rho^2 c R \bar{w}^2 U^4/(r_o^2 c_o^2) \tag{10}$$

To evaluate the scaling factor $K_1(f)$, the wind turbine rotor has been modeled as a dipole point source located at the hub and Eq. (10) is compared with frequency spectra from the MOD-2 machine for which the noise was largely due to turbulent inflow.[12,13] The location of the peak intensity in the frequency domain is strongly dependent on blade velocity

and longitudinal scale of turbulence.[25] The turbulence is dependent on the height above the ground for nonvarying meteorological conditions. To account for different hub heights as well as different rotor diameters, the location of the peak intensity in the frequency domain is given by

$$f_{\text{peak}} = SU/(h-0.7R) \tag{11}$$

where $S$ is the applicable Strouhal number obtained from the measured MOD-2 noise spectra.

*Power Output and Wind Speed*

If the power generated by the wind turbine is known rather than the wind speed, which is needed as input for Eqs. (4) and (5), it is necessary to know their relationship to enable noise predictions. The lift force $L$ produced by an airfoil section at angle of attack $\alpha$ can be expressed as

$$L = (\rho/2)U^2(\mathrm{d}C_L/\mathrm{d}\alpha)\alpha c \tag{12}$$

where the lift curve slope $dC_L/\mathrm{d}\alpha$ is approximately constant throughout the range of $\alpha$ below the stall angle. The relation between the angle of attack $\alpha$, the aerodynamic pitch angle $\gamma$, and the geometric pitch angle $\beta$ is defined by

$$\alpha = \gamma - \beta \tag{13}$$

For constant rotational speed, it is assumed that the increase in torque $\mathrm{d}Q$, due to an increasing wind speed between cut-in and rated, is given by

$$\mathrm{d}Q = B\Delta L \sin\gamma r_x \mathrm{d}r_x \tag{14}$$

The increase in torque, which is not needed to maintain the constant rotational speed, is used to generate electrical power. The power extracted from the wind is then proportional to

$$P \equiv Q\dot{\theta} \tag{15}$$

When the wind speed $V_w$ exceeds the cut-in speed $V_{ci}$, the aerodynamic pitch angle is increased. The increase in angle of attack is then given by

$$\Delta\alpha = \Delta\gamma - \beta = (V_w - V_{ci})/U - \beta \tag{16}$$

Combining Eqs. (12), (14), and (16) and integrating over the blade yields the proportion of the total torque extracted from the wind that is not needed to keep the wind turbine at constant rotational speed,

$$Q \equiv \beta(\rho/2)(V_w - V_{ci} - \beta U)V_w R^2 c \tag{17}$$

Substituting Eq. (17) into Eq. (15) yields for the extracted power

$$P \equiv (V_w - V_{ci} - \beta U)V_w \tag{18}$$

and for the power ratio

$$P/P_r = (V_w - V_{ci} - \beta U)V_w/[(V_r - V_{ci} - \beta U)V_r] \tag{19}$$

Solving Eq. (19) for the wind speed $V_w$ yields a function of output power $P$ and other constants that vary for each different wind turbine,

$$V_w = 0.5\left\{V_{ci} + \beta U + \left[(V_{ci} + \beta U)^2 + 4\frac{P}{P_r} \times V_r(V_r - V_{ci} - \beta U)\right]^{1/2}\right\} \tag{20}$$

Equation (20) shows that for rated power output the rated wind speed is obtained, while for zero power output the wind speed equals cut-in.

**Turbulent Boundary-Layer/Trailing-Edge Interaction**

Noise is generated when the blade-attached turbulent boundary layers convect into the wake at the trailing edge. Theoretical models of this trailing-edge noise for helicopter blades are presented in Refs. 22, 23, and 43-53. The experimental and theoretical study in Ref. 47 concludes that the trailing-edge noise radiated from a local blade segment can be predicted by a first principles theory, which includes local Mach number, boundary-layer thickness, length of the blade segment, and observer position. A scaling law approach then was used for comparison with the noise radiation data from a stationary two-dimensional isolated airfoil segment. This theory will be utilized to predict the trailing-edge noise generated by the blades of horizontal axis wind turbine generators.

The scaling law prediction of Ref. 47 gives for the trailing-edge noise spectrum of an isolated airfoil

$$\mathrm{SPL}_{1/3} = 10\log\left\{K_2 U^5 B\bar{D}\frac{\delta s}{r_o^2}\left(\frac{S}{S_{\max}}\right)^4 \times\left[\left(\frac{S}{S_{\max}}\right)^{1.5} + 0.5\right]^{-4}\right\} \tag{21}$$

where $K_2$ equals 3.5 when SI units are used. Equation (21) is essentially the trailing-edge noise prediction for a two-dimensional lifting surface in a uniform inflow. To predict the trailing-edge noise from a rotating blade, the blade is divided into small blade segments of length $\ell$, each experiencing a different local freestream velocity and each contributing to the noise at the receiver location. Because of the rotor rotation, this noise spectrum then is averaged around the azimuth. The local freestream velocity $U_x$ is given by

$$U_x = 2\pi r_x n \tag{22}$$

The thickness of the turbulent boundary layer at the trailing edge of the airfoil may be approximated by the turbulent boundary-layer thickness of a flat plate, which is given by[54]

$$\delta_x = 0.37c_x/(R_{N_x})^{0.2} \tag{23}$$

Assuming a linearly tapered rotor blade and neglecting twist, the local chord $c_x$ can be expressed in terms of the root chord $c_r$, tip chord $c_t$, radius $r_x$, and blade diameter $D$,

$$c_x = c_t + (1 - 2r_x/D)(c_r - c_t) \tag{24}$$

The local Reynolds number is defined by

$$R_{N_x} = U_x c_x/\nu \tag{25}$$

The directivity pattern of the radiated trailing-edge noise for a source and a receiver in the vertical on-axis plane is given by dipole-like behavior from Ref. 47,

$$\bar{D}\left(\theta, \frac{\pi}{2}\right) = \frac{\sin^2(\theta/2)}{(1+M\cos\theta)[1+(M-M_c)\cos\theta]^2} \tag{26}$$

The convection Mach number of the turbulence ($M_c$) is set to an average value of 0.8 $M$ as suggested in Ref. 47. To correct for the directivity of the source outside the vertical on-axis plane, the source is assumed to be a dipole radiator in those directions and the directivity function is the one proposed by Fink,[55]

$$\bar{D}(\theta,\psi) = \sin^2\psi\bar{D}[\theta,(\pi/2)] \tag{27}$$

The Strouhal number in Eq. (21) is defined as

$$S = f\,\delta/U \tag{28}$$

The peak Strouhal number $S_{max}$ associated with trailing-edge noise equals 0.1.[47,55] Although a different value is reported in Ref. 40, in the present study a value $S_{max} = 0.1$ is adopted.

**Trailing-Edge Bluntness Vortex Shedding Noise**

Vortex shedding behind the trailing edges of thick struts has been studied in Ref. 48. This phenomenon produces noise as the coherent vortex shedding causes a fluctuating surface pressure differential across the trailing edge. This was established in Ref. 46 as being an important source of self-noise for airfoils with blunt trailing edges. The vortex shedding frequencies observed in Ref. 48 had a peak Strouhal number of about 0.25 when based on the trailing-edge thickness and a velocity dependence of approximately $U^6$. This peak Strouhal number compares well with the ones found by other researchers who studied the vortex shedding behind wings, flat plates, and circular and noncircular bodies.[24,43,46,49-52] In all cases, the turbulent boundary-layer displacement thickness $\delta^*$ is much smaller than the characteristic dimension $t$ from which the vorticies are shed ($t/\delta^* > 40$). However, experimental results from noise measurements on several trailing-edge configurations in the NASA Langley Quiet-Flow Facility indicated that for a trailing-edge bluntness of equal thickness or smaller than the displacement thickness of the boundary layer a Strouhal number of 0.1 is applicable.[46] It was shown that the overall sound pressure level of the noise generated at the blunt trailing edge follows a $U^{5.3}$ dependence. Using the directivity pattern presented in Ref. 53, the following scaling laws are derived for the one-third octave band sound pressure levels in the acoustic far field.

For $t/\delta^* > 1.3$:

$$\mathrm{SPL}_{1/3} = 10\log\left[\frac{K_3(f)BU^6 ts\,\sin^2\theta\sin^2\psi}{(1+M\cos\theta)^6 r_o^2}\right] \tag{29}$$

and

$$f_{max} = \frac{0.25U}{t+\delta/4} \tag{30}$$

For $t/\delta^* < 1.3$:

$$\mathrm{SPL}_{1/3} = 10\log\left[\frac{K_4(f)BU^{5.3} ts\,\sin^2(\theta/2)\sin^2\psi}{(1+M\cos\theta)^3\,[1+(M-M_c)\cos\theta]^2 r_o^2}\right] \tag{31}$$

and

$$f_{max} = 0.1U/t \tag{32}$$

The frequency dependent constant $K_4(f)$ has been obtained by comparing Eq. (31) with the blunt trailing-edge noise measurements from Fig. 40 in Ref. 46, which were first converted to one-third octave band data. The frequency dependent constant $K_3(f)$ has been determined by equating Eqs. (29) and (31) for the case in which the trailing-edge bluntness is 1.3 times the displacement thickness of the turbulent boundary layer. For most practical purposes, the displacement thickness and the boundary-layer thickness are related by

$$\delta^* = \delta/8 \tag{33}$$

Equations (29-33) are used to predict noise from wind turbine blades with blunt trailing edges using the same calculation procedure as for turbulent boundary-layer/trailing-edge interaction noise.

To assess the relative importance of all three major aerodynamic noise sources (Fig. 1), predictions have been made for a MOD-2 machine at a distance of 100 m on-axis. The noise contributions due to turbulent inflow, trailing-edge bluntness, and turbulent boundary-layer/trailing-edge interaction relative to the total noise is depicted in Fig. 2. The turbulent inflow-related noise dominates the spectrum at the low frequencies and is broad in character, while turbulent boundary-layer/trailing-edge interaction noise becomes relatively more and more important when moving up the frequency scale. Noise due to trailing-edge bluntness is confined to a more restricted frequency band, with its center frequency related to the thickness of the trailing edge. All predictions are limited to the acoustic far field, on-axis and without distinction between upwind and downwind directions as no propagation effects are incorporated.

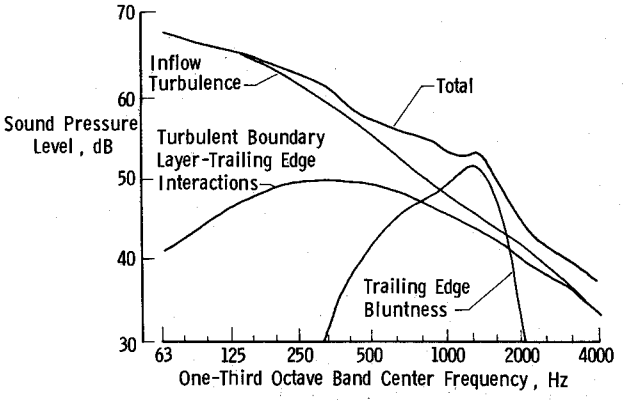


**Fig. 2 On-axis broadband noise component predictions for the MOD-2 machine ($V_w = 9.8$ m/s, $P = 1500$ kW, $r_o = 100$ m).**

## Noise Measurements

Acoustic measurements are available for four different, currently operating, horizontal axis wind turbine generators.[11-13,17-21] They consist of one upwind machine (the MOD-2) on which the rotor is located upwind from the supporting tower and three downwind machines (MOD-OA, WTS-4, and U.S. Windpower Inc. machine) as depicted in Fig. 3. The first three are government sponsored. All are self-starting, have two or three blades, and normally operate at wind speeds of 3-16 m/s. Some dimensions and operational details are included in Table 1. Receiver locations range from 18-800 m and are considered to be in the acoustic far field. Measurements were made with a windscreen-covered microphone, positioned close to the ground, to minimize the adverse effects of the wind blowing over the microphone.

## Comparison between Predictions and Measurements

Predictions and measurements are compared for mean acoustic emission levels on the basis of one-third octave bands for the machines shown in Fig. 1 and described in Table 1. The frequency range of interest for wind turbine broadband noise covers the 63-4000 Hz one-third octave bands. A-weighted levels outside this range are of lesser importance for community noise acceptance. To show that reasonable agreement can be obtained between noise prediction and far-field, downwind, noise measurements, comparisons have been made for the four machines under quite different operating conditions and at different measurement locations (Figs. 4-7). In general, predictions are within 4 dB of the measurement data. This agreement is quite acceptable considering the vastly different physical and geometric characteristics of the wind turbines and the other parameters involved. To investigate some of these parameters, comparisons have been made to establish the effects of upwind and downwind receiver location, power output, distance from the machine, and bluntness of the blade trailing edge.

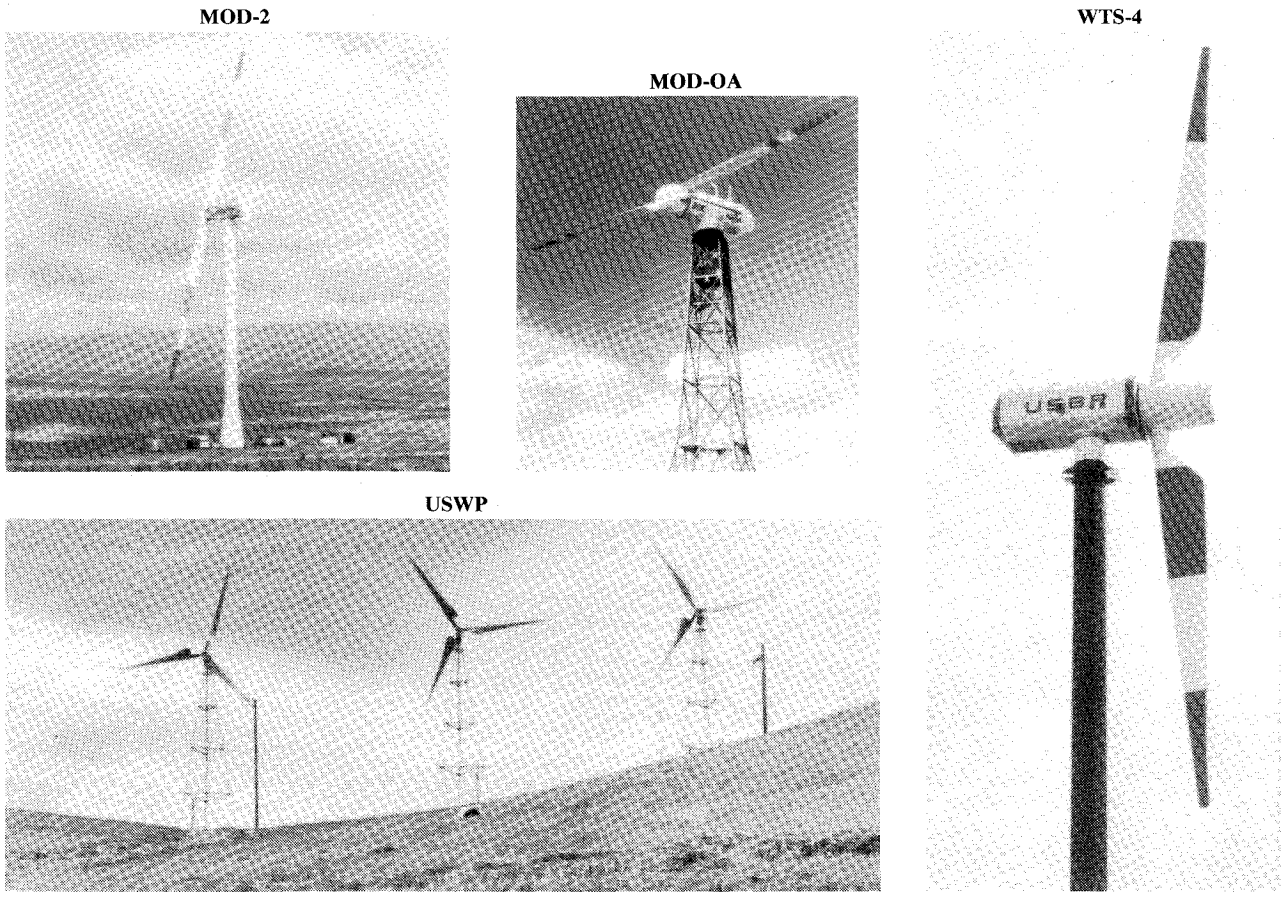


Fig. 3 Wind turbine generators for which predictions are compared with measurements.

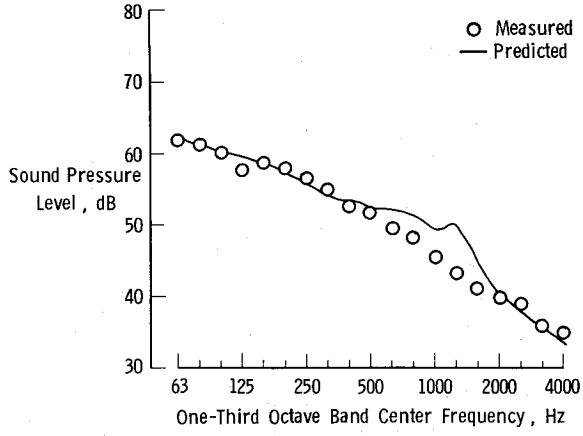


Fig. 4 Measured and predicted broadband noise spectra for the MOD-2 machine ($P = 1000$ kW, $r_o = 150$ m).

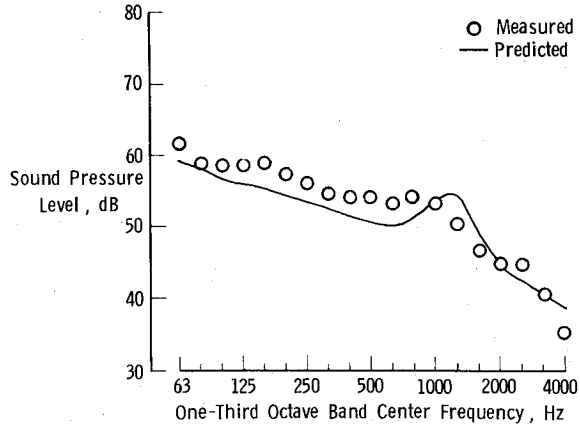


Fig. 5 Measured and predicted broadband noise spectra for the MOD-OA machine ($P = 70$ kW, $r_o = 60$ m).

Table 1 Wind turbine design specifications

| Designation | MOD-OA | MOD-2 | WTS-4 | U.S. Windpower (USWP) |
|---|---|---|---|---|
| Rated power, kW | 200 | 2500 | 4000 | 50 |
| Rotor location | Downwind | Upwind | Downwind | Downwind |
| Rotations/min | 40.0 | 17.5 | 30.0 | 72.0 |
| No. of blades | 2 | 2 | 2 | 3 |
| Tip speed, m/s | 80.0 | 83.8 | 122.4 | 66.5 |
| Rotor diameter, m | 38.1 | 91.4 | 78.4 | 17.1 |
| Hub height, m | 30.5 | 61.0 | 80.0 | 18.3 |
| Blade area, $m^2$ | 28 | 236 | 195 | 15 |

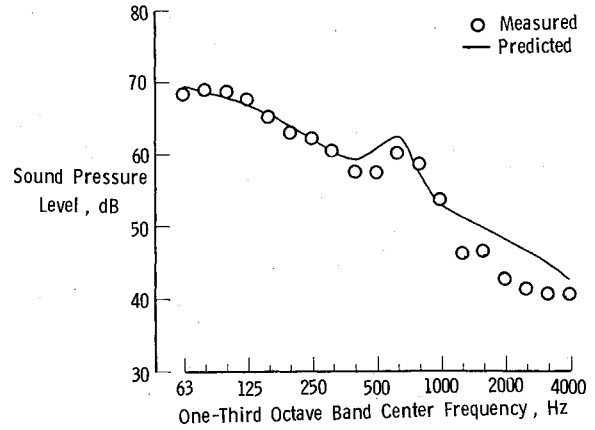


**Fig. 6 Measured and predicted broadband noise spectra for the WTS-4 machine ($P=2500$ kW, $r_o=200$ m).**

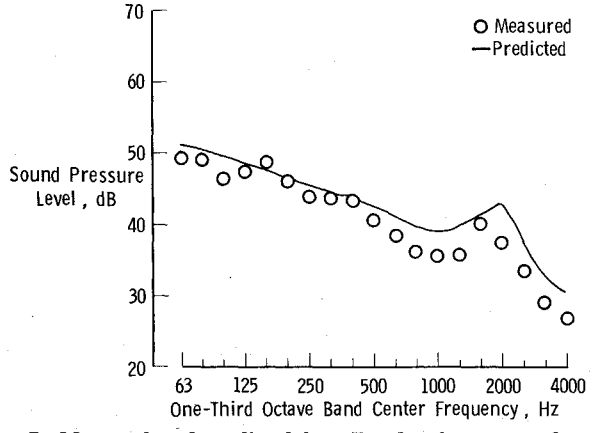


**Fig. 7 Measured and predicted broadband noise spectra for the U. S. Windpower Inc. machine ($P=25$ kW, $r_o=91$ m).**

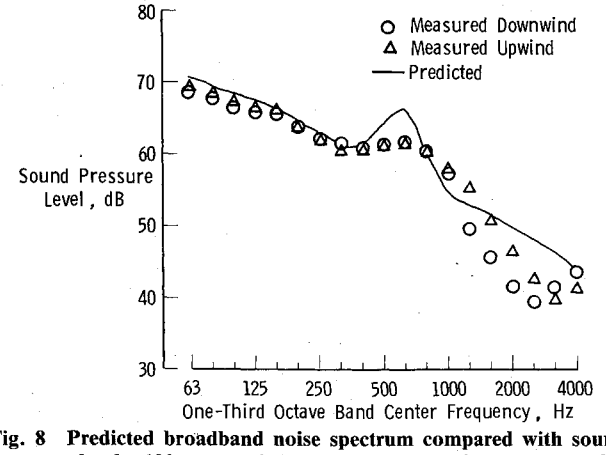


**Fig. 8 Predicted broadband noise spectrum compared with sound pressure levels 100 m upwind and downwind from the WTS-4 machine ($P=2500$ kW).**

### Directivity

The broadband noise predictions in this paper are limited to on-axis receiver locations. Comparing upwind and downwind measured acoustic data at equal distances from the machines, essentially no differences are observed in either spectral shape or sound level (Fig. 8). The predictions are thus valid for upwind or downwind receiver locations. However, this is true only for close-in measurement locations in the acoustic far field since no propagation effects are included. The formation of a shadow zone upwind due to the refraction effects of the mean wind speed gradient, propagation enhancement downwind, and atmospheric and ground absorption will affect sound pressure levels at greater distances from the machine.

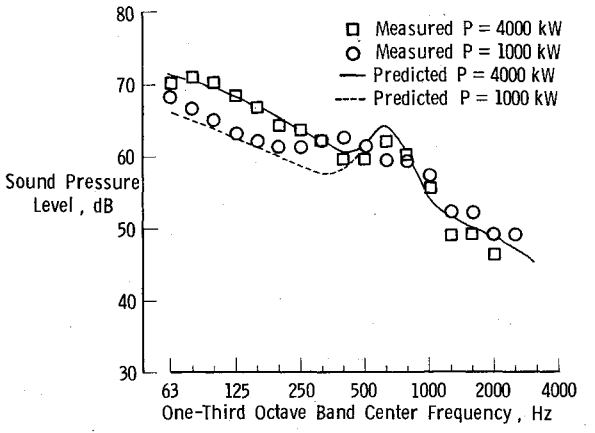


**Fig. 9 Effect of output power (wind speed) on the measured and predicted broadband noise spectra of the WTS-4 machine ($r_o=150$ m).**

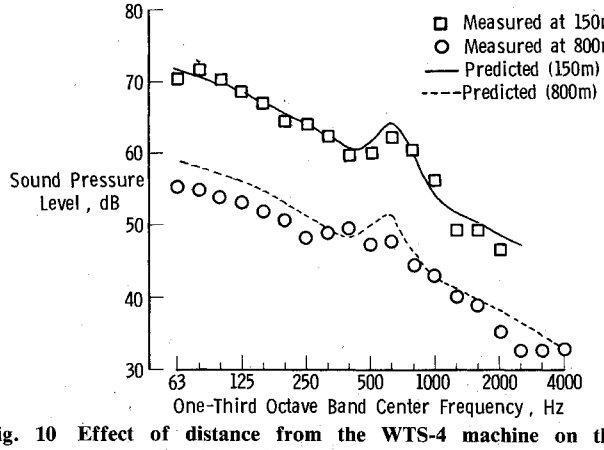


**Fig. 10 Effect of distance from the WTS-4 machine on the measured and predicted broadband noise spectra ($P=4000$ kw).**

### Output Power

It was assumed in the theoretical analysis of the noise due to inflow turbulence that the root mean square turbulence intensity is a function of only wind speed and height above the ground [Eq. (5)]. The sound power for this noise source (Fig. 1) and the electrical power output are dependent on the wind speed (between cut-in and rated). Figure 9 shows the predicted and measured broadband noise spectra at 150 m distance from the WTS-4 machine for two output power conditions. In the case of constant-rotational machines, noise source mechanisms other than inflow turbulence are independent of wind speed, as evidenced in Fig. 9.

### Distance

The one-third octave band spectra of the WTS-4 and U.S. Windpower Inc. wind turbines in Figs. 10 and 11 illustrate the effects of distance from the machines. All measured and predicted data points are for downwind on-axis locations. Some differences between the measured and predicted sound pressure levels for the 800 m receiver location in Fig. 10 are due to propagation effects that are not included in the prediction method.

In Fig. 11, the lower prediction curve and corresponding measured data are adjusted to 50 kW output power from the 25 kW for which measurements were available. The distance square relationship for all noise mechanisms [Eqs. (10), (21), and (31)] suggest a 14 dB decrease in sound pressure levels when extending the receiver location from 18 to 91 m. The observed decrease in measured sound pressure levels of 6-9

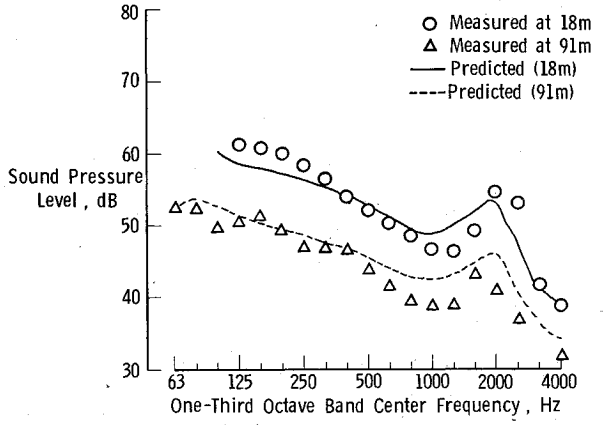


**Fig. 11 Effect of distance from the U.S. Windpower Inc. machine on the measured and predicted broadband noise spectra ($P=50$ kW).**

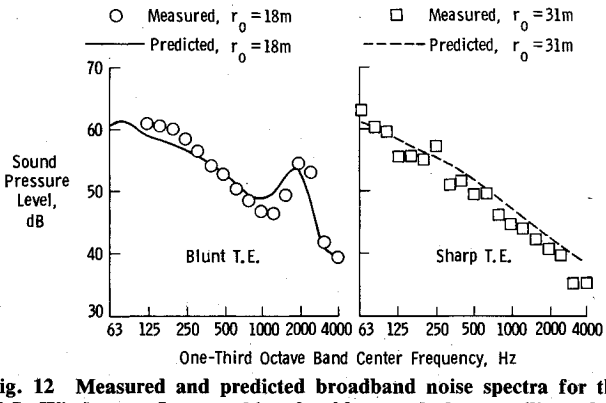


**Fig. 12 Measured and predicted broadband noise spectra for the U.S. Windpower Inc. machine for blunt and sharp trailing edges ($P=50$ kW).**

dB is due to the dipole-like behavior of the noise source mechanisms and is well approximated by the predictions.

#### Trailing-Edge Bluntness

The trailing-edge bluntness vortex shedding noise is a source mechanism not considered earlier as a major contributor for helicopter or wind turbine noise. Experimental data were available from measurements on isolated airfoils and its effect is clearly illustrated in Fig. 12. Measurements and predictions are shown for the U.S. Windpower Inc. machine for which the blades have blunt trailing edges. The peak in the measured noise spectrum around 2000 Hz is well predicted. Also shown is the noise spectrum of the U.S. Windpower Inc. machine with the blade trailing edges sharpened, which results in elimination of the 2000 Hz peak. Reasonable agreement between measurements and predictions has been obtained.

## Conclusions

A method has been presented for predicting the broadband noise spectra of horizontal axis, constant-rotational-speed wind turbine generators. The analysis is based on the contributions of such noise mechanisms as inflow turbulence, turbulent boundary-layer/trailing-edge interaction, and noise due to a blunt trailing edge. Good agreement is shown between predictions and far-field noise measurements of four wind turbine generators under various operating conditions. The prediction method includes the effects of distance from the machine, output power (wind speed), number of blades, and tower and blade geometry. Broadband noise is predicted only on-axis and the method does not distinguish between upwind and downwind. Propagation effects other than distance are not included in the present prediction formulation.

## Acknowledgments

This research has been supported by the NASA Langley Research Center under Contract NAS1-16978, Dr. C. A. Powell, Technical Monitor.

## References

[1]Stephens, D. G., Shepherd, K. P., Hubbard, H. H., and Grosveld, F. W., "Guide to the Evaluation of Human Exposure to Noise from Large Wind Turbines," NASA TM 83288, March 1982.

[2]Shepherd, K. P., Grosveld, F. W., and Stephens, D. G., "Evaluation of Human Exposure to the Noise from Large Wind Turbine Generators," *Noise Control Engineering Journal*, Vol. 21, Jan. 1983, pp. 30-37.

[3]Balombin, J. R., "An Exploratory Survey of Noise Levels Associated with a 100 kW Wind Turbine," NASA TM 81486, April 1980.

[4]Greene, G. C. and Hubbard, H. H., "Some Calculated Effects of Non-Uniform Inflow on the Radiated Noise of a Large Wind Turbine," NASA TM 81813, May 1980.

[5]Kelley, N. D., "Acoustic Noise Generation by DOE/NASA MOD-1 Wind Turbine," NASA CP 2185, Feb. 1981.

[6]Martinez, R., Widnall, S. E., and Harris, W. L., "Predictions of Low-Frequency Sound from the MOD-1 Wind Turbine," Massachusetts Institute of Technology, Cambridge, FDL Rept. 80-5, 1980, p. 77.

[7]Savino, J. M., Wagner, L. H., and Sinclair, D. M., "Wake Characteristics of an Eight-Leg Tower for a MOD-0 Type Wind Turbine," U.S. Department of Energy, Rept. DOE/NASA 1038-77/14, Dec. 1977.

[8]Thomson, D. W. and Roth, S. D., "Enhancement of Far-Field Sound Levels by Refractive Focussing," NASA CP 2185, Feb. 1981.

[9]Wells, R. J., "GE MOD-1 Noise Study," NASA CP 2185, Feb. 1981.

[10]Viterna, L. A., "The NASA LeRC Wind Turbine Sound Prediction Code," NASA CP 2185, Feb. 19, 1981.

[11]Grosveld, F. W., Shepherd, K. P., and Hubbard, H. H., "Radiation of Aerodynamic Sound from Large Wind Turbine Generators," *Proceedings of Inter-Noise '82,* Noise Control Foundation, Poughkeepsie, N. Y., Vol. 1, May 1982, p. 323.

[12]Hubbard, H. H., Shepherd, K. P., and Grosveld, F. W., "Sound Measurements of the MOD-2 Wind Turbine Generator," NASA CR 165752, July 1981.

[13]Hubbard, H. H., Grosveld, F. W., and Shepherd, K. P., "Noise Characteristics of Large Wind Turbine Generators," *Noise Control Engineering Journal*, Vol. 21, Jan. 1983, pp. 21-29.

[14]Keast, D. N. and Potter, R. C., "A Preliminary Analysis of the Audible Noise of Constant Speed, Horizontal-Axis Wind Turbine Generators," U.S. Department of Energy, Rept. DOE/EV-0089, UC-11, Pt. 60, July 1980.

[15]Kelley, N. D., "A Methodology for Assessment of Wind Turbine Noise Generation," Solar Energy Research Institution, SERI/CP 635 1340, Oct. 1981, (available from NTIS, DOC, Springfield, Va.).

[16]George, A. R. and Chou, S. T., "Comparison of Broadband Noise Mechanisms, Analyses, and Experiments on Helicopters, Propellers, and Wind Turbines," AIAA Paper 83-0690, April 1983.

[17]Shepherd, K. P. and Hubbard, H. H., "Sound Measurements and Observations of the MOD-OA Wind Turbine Generator," NASA CR 165856, Feb. 1982.

[18]Shepherd, K. P. and Hubbard, H. H., "Measurements and Observations of Noise from a 4.2 Megawatt (WTS-4) Wind Turbine Generator," NASA CR 166124, May 1983.

[19]Hubbard, H. H. and Shepherd, K. P., "Noise Measurements for Single and Multiple Operation of 50 kW Wind Turbine Generators," NASA CR 166052, Dec. 1982.

[20]Grosveld, F. W., Shepherd, K. P., and Hubbard, H. H., "Measurement and Prediction of Broadband Noise from Large Horizontal Axis Wind Turbine Generators," *Proceedings of NASA/DOE Workshop on Horizontal Axis Wind Turbine Technology*, May 1984.

[21]Grosveld, F. W., "Prediction of Broadband Noise from Large Horizontal Axis Wind Turbine Generators," AIAA Paper 84-2357, Oct. 1984.

[22]George, A. R., "Helicopter Noise: State of the Art," *Journal of Aircraft*, Vol. 15, Nov. 1978, pp. 707-715.

[23]Schlinker, R. H. and Brooks, T. F., "Progress in Rotor Broadband Noise Research," American Helicopter Society Paper A-82-38-51-D, May 1982.

[24]Berger, E. and Wille, R., "Periodic Flow Phenomena," *American Review of Fluid Mechanics*, Vol. 4, 1972, p. 313.

[25]Aravamudan, K. S., Lee, A., and Harris, W. L., "A Simplified

Mach Number Scaling Law for Helicopter Rotor Noise," *Journal of Sound and Vibration*, Vol. 57, No. 4, 1978, pp. 555-570.

[26]Amiet, R. K., "Noise Due to Rotor-Turbulence Interaction," NASA CP 2052, May 1978.

[27]Osborne, C., "Unsteady Thin Airfoil Theory for Subsonic Flow," *AIAA Journal*, Vol. 11, Feb. 1973, pp. 205-209.

[28]Ffowcs Williams, J. E. and Hawkings, D. L., "Theory Relating to the Noise of Rotating Machinery," *Journal of Sound and Vibration*, Vol. 10, 1969, pp. 10-21.

[29]Whitfield, C. E., "An Investigation of Rotor Noise Generation by Aerodynamic Disturbance," NASA CR 157471, 1977.

[30]Leverton, J. W., "The Noise Characteristics of a Large 'Clean' Rotor," *Journal of Sound and Vibration*, Vol. 27, No. 3, April 1973, pp. 357-376.

[31]Homicz, G. F. and George, A. R., "Broadband and Discrete Frequency Radiation from Subsonic Rotors," *Journal of Sound and Vibration*, Vol. 36, No. 2, Sept. 1974, pp. 151-178.

[32]Hayden, R., "Noise from Interaction of Flow with Rigid Surfaces: A Review of Current Status of Prediction Techniques," NASA CR 2126, Oct. 1972.

[33]Lowson, M. V. and Ollerhead, J. B., "A Theoretical Study of Helicopter Rotor Noise," *Journal of Sound and Vibration*, Vol. 9, March 1969, pp. 197-222.

[34]Lowson, M. V., Whatmore, A. R., and Whitfield, C. E., "Source Mechanisms for Rotor Noise Radiation," NASA CR 2077, Aug. 1973.

[35]Paterson, R. W. and Amiet, R. K., "Noise of a Model Helicopter Rotor Due to Ingestion of Turbulence," NASA CR 3213, Nov. 1979.

[36]Humbad, N. G. and Harris, W. L., "Model Rotor Low Frequency Broadband Noise at Moderate Tip Speeds," AIAA Paper 80-1013, June 1980.

[37]George, A. R. and Kim, Y. N., "High Frequency Broadband Rotor Noise," *AIAA Journal*, Vol. 15, April 1977, pp. 538-545.

[38]Piercy, J. E., Embleton, T. F., and Sutherland, L. C., "Review of Noise Propagation in the Atmosphere," *Journal of the Acoustical Society of America*, Vol. 61, June 1977, pp. 1403-1418.

[39]Ingard, U., "The Physics of Outdoor Sound," *Proceedings of the 4th National Noise Abatement Symposium,* National Noise Abatement Council, New York, N.Y., 1953, pp. 11-25.

[40]Boeing Engineering and Construction, "MOD-2 Wind Turbine System Concept and Preliminary Design Report," U.S. Department of Energy, Rept. DOE/NASA 0002-80/2, July 1979.

[41]Lighthill, M. J., "On Sound Generated Aerodynamically; General Theory," *Proceedings of the Royal Society of London*, Vol. A211, 1952, pp. 564-587.

[42]Curle, N., "The Influence of Solid Boundaries upon Aerodynamic Sound," *Proceedings of the Royal Society of London*, Vol. A231, 1955, pp. 505-514.

[43]Chase, D. M., "Noise Radiated from an Edge in Turbulent Flow," *AIAA Journal*, Vol. 13, Aug. 1975, pp. 1041-1047.

[44]Amiet, R. K., "Effect of the Incident Surface Pressure Field on Noise Due to Turbulent Flow Past a Trailing Edge," *Journal of Sound and Vibration*, Vol. 57, 1978, pp. 305-306.

[45]Yu, J. D. and Tam, C. K., "An Experimental Investigation of the Trailing Edge Noise Mechanism," *AIAA Journal*, Vol. 16, Oct. 1978, pp. 1045-1052.

[46]Brooks, T. F. and Hodgson, T. H., "Prediction and Comparison of Trailing Edge Noise Using Measured Surface Pressures," AIAA Paper 80-0977, June 1980.

[47]Schlinker, R. H. and Amiet, R. K., "Helicopter Rotor Trailing Edge Noise," NASA CR 3470, Nov. 1981.

[48]Blake, W. K., "A Statistical Description of Pressure and Velocity Fields at the Trailing Edges of a Flat Strut," David W. Taylor Naval Ship R&D Center, Rept. 4241, Dec. 1975.

[49]Krzywoblocki, M. Z., "Investigation of the Wing-Wake Frequency with Application of the Strouhal Number," *Journal of the Aeronautical Sciences*, Vol. 12, Jan. 1945, pp. 51-62.

[50]Mendenhall, M. R., Spangler, S. B., and Perkins, S. C. Jr., "Vortex Shedding from Circular and Non-Circular Bodies at High Angles of Attack," AIAA Paper 79-0026, Jan. 1979.

[51]Nishioka, M. and Sato, H., "Mechanism of Determination of the Shedding Frequency of Vortices Behind a Cylinder at Low Reynolds Numbers," *Journal of Fluid Mechanics*, Vol. 89, 1978, pp. 49-60.

[52]Katz, J. and Weihs, D., "Behavior of Vortex Wakes from Oscillating Airfoils," *Journal of Aircraft*, Vol. 15, Dec. 1978, pp. 861-863.

[53]Howe, M. S., "A Review of the Theory of Trailing Edge Noise," *Journal of Sound and Vibration*, Vol. 61, No. 3, Dec. 1978, pp. 437-465.

[54]Schlichting, H., *Boundary Layer Theory* (6th ed.) McGraw-Hill Book Co., New York, 1968.

[55]Fink, M. R., "Noise Component Method for Airframe Noise," *Journal of Aircraft*, Vol. 16, Oct. 1979, pp. 659-665.